Biochimica et Biophysica Acta 1850 (2015) 802–812

Contents lists available at ScienceDirect

Biochimica et Biophysica Acta

journal homepage: www.elsevier.com/locate/bbagen

Chip physically interacts with Notch and their stoichiometry is critical for Notch function in wing development and cell proliferation in *Drosophila*

Nalani Sachan [1], Abhinava K. Mishra, Mousumi Mutsuddi, Ashim Mukherjee *

Department of Molecular and Human Genetics, Banaras Hindu University, Varanasi 221 005, India

ARTICLE INFO

Article history:
Received 26 September 2014
Received in revised form 15 December 2014
Accepted 27 December 2014
Available online 15 January 2015

Keywords:
Drosophila
Notch
Chip
dorso-ventral boundary
cell proliferation

ABSTRACT

Background: Notch signaling plays a fundamental role both in metazoan cell fate determination and in the establishment of distinct developmental cell lineages. In a yeast two-hybrid screen, we identified Chip as a binding partner of Notch. Thus, we investigated the functional significance of Notch and Chip interactions.
Methods: Co-immunoprecipitation and GST pull-down experiments confirmed the physical interaction between Notch and Chip. Immunostaining revealed that Chip and Notch-intracellular domain (Notch-ICD) co-localized in cell nuclei. Loss-of-function and gain-of-function analyses of *Chip* were carried out using FLP/FRT and *GAL4-UAS* systems, respectively. Immunostaining and real-time PCR were performed to analyze the role of Chip on Notch-induced cell proliferation.
Results: Here, we report transcriptional cofactor Chip as a novel binding partner of Notch. Chip and Notch also showed strong genetic interactions, and *Chip* mutant clones in the dorsal compartment induced ectopic wing margins by ectopic expression of Notch and its targets, Wg and Cut. Our analyses revealed that stoichiometry of Notch and Chip is critical at the dorso-ventral (DV) boundary for wing margin formation. In addition, overexpression of Chip can rescue Notch-induced cell proliferation in larval imaginal discs.
Conclusions: Our results indicate that Notch function in the DV boundary area is presumably dependent on Notch–Chip heterodimer formation. In addition, overexpression of Chip can rescue Notch-induced cell proliferation, presumably through titration of overexpressed Notch-ICD by excess Chip molecules.
General Significance: The present study reveals that Chip is a novel interacting partner of Notch and it plays a major role in Notch-induced DV margin formation and cell proliferation.

1. Introduction

Notch signaling is an evolutionarily conserved pathway that operates to influence an astonishing array of cell fate decisions in different developmental contexts. Being pleiotropic in nature, the Notch function affects differentiation, proliferation, apoptotic events, and self-renewal processes of different tissues [1–5]. The Notch mutant was isolated almost a century ago as a dominant X-linked mutation that exhibits a notched wing margin phenotype in *Drosophila melanogaster*; hence, the name Notch was given for this gene [6,7]. The loss of Notch function in *Drosophila* embryo leads to a massive overproduction of neurons at the expense of the epidermis and generates the 'Neurogenic' phenotype. The central element of the pathway is the Notch receptor, which displays exceptional sensitivity to gene dosage. Notch was first cloned in *Drosophila*, and molecular characterization revealed that the Notch gene encodes a transmembrane surface receptor [8]. The Notch receptor is synthesized as a single 300 kDa polypeptide precursor, which is cleaved by furin-like convertase in the trans-Golgi compartment to form an N-terminal extracellular subunit and a C-terminal transmembrane intracellular subunit [9]. This heterodimeric receptor is then transferred to the cell membrane and it interacts with ligands of the DSL family (Delta and Serrate/Jagged in *Drosophila* and mammals and LAG-2 in *C. elegans*). Binding of ligands to extracellular domain leads to proteolytic cleavages by metalloproteases and γ-secretase, and this in turn results in the release of Notch intracellular domain [10–13]. The Notch intracellular domain (Notch-ICD) binds to Importin-α3 and is translocated to the nucleus using the canonical Importin-α3/Importin-β transport pathway [14]. The Notch-ICD directly participates in a transcriptional complex involving CSL transcription factor (mammalian CBF1/*Drosophila* suppressor of hairless/*C. elegans* LAG-1) and transcriptional co-activators like Mastermind (Mam), leading to activation of Notch target genes such as the enhancer of split [*E*(*spl*)] complex genes, which encodes bHLH transcription factors that in turn repress Achaete-Scute complex (As-C) proneural genes [15–17]. The deployment of Notch signaling pathway in numerous cellular contexts to influence varied aspects of development is possible due to its multiple levels of regulation by which appropriate signaling outputs in a variety of cellular

* Corresponding author at: Department of Molecular and Human Genetics, Banaras Hindu University, Varanasi 221 005, India. Tel.: +91 542 6702490; fax: +91 542 2368457.
E-mail address: ashim04@gmail.com (A. Mukherjee).
[1] Present address: The Stowers Institute for Medical Research, Kansas City, Missouri 64110, USA.

http://dx.doi.org/10.1016/j.bbagen.2014.12.026
0304-4165/

contexts are generated [3,4,18,19]. Several recent genome-wide studies in *D. melanogaster* have revealed a vast network of genes that can affect Notch signaling activity and its integration and cross-talk with other signaling pathways (reviewed in ref. [4]).

In a yeast two-hybrid screen, we identified Chip/dLdb, previously reported as a cofactor of Apterous (Ap), as a binding partner of Notch. The LIM homeodomain (LIM-HD) transcription factor Ap contains one homeodomain and two LIM domains [20,21]. In the *Drosophila* wing, *apterous* (*ap*) functions as a dorsal selector gene [22–24]. In order to control DV patterning and the growth of *Drosophila* wing, Ap needs the activity of its cofactor Chip/dLdb, which is a *Drosophila* ortholog of the vertebrate LDB/NL1/CLIM-2 proteins [25–27]. Chip has a self-interacting dimerization domain (DD) and a LIM-interaction domain (LID) that binds to the LIM domains of Ap and other proteins [28]. Complex formation between Ap, Chip, and DNA stabilizes Ap protein *in vivo* [29]. Chip is expressed throughout development and is present in the nuclei of cells in embryo, larval brain, imaginal discs, fat body, and salivary glands [25,26]. Although the nuclear protein Chip is expressed in both dorsal and ventral cells of the wing imaginal disc, somatic clonal analysis revealed that it has no role in ventral cells [25]. Both loss as well as excess of *Chip* function in the dorsal compartment of the wing discs causes the same phenotype as *ap* loss-of-function phenotype such as generation of ectopic wing margins and wing outgrowths without affecting normal accumulation of Ap protein [25]. Moreover, the *Chip* gain-of-function phenotype can be rescued by *ap* overexpression [25,27]. The correct amount of Chip is a prerequisite for normal function of Ap in DV compartmentalization in the wing. It has been shown further that overexpression of *Chip-ΔDD* mutant construct causes *ap* lack-of-function phenotypes similar to those caused by overexpression of wild-type *Chip*, and these phenotypes can be rescued by simultaneous overexpression of *ap*. Actually, *Chip-ΔDD* overexpression phenotypes are caused by titration of Ap because these phenotypes can be rescued by adding extra Ap. On the contrary, phenotypes caused by overexpression of *Chip-ΔLID* cannot be rescued by simultaneous overexpression of *ap* because this mutant interferes with the formation of functional tetramer. Based on these evidences, the model that the Ap

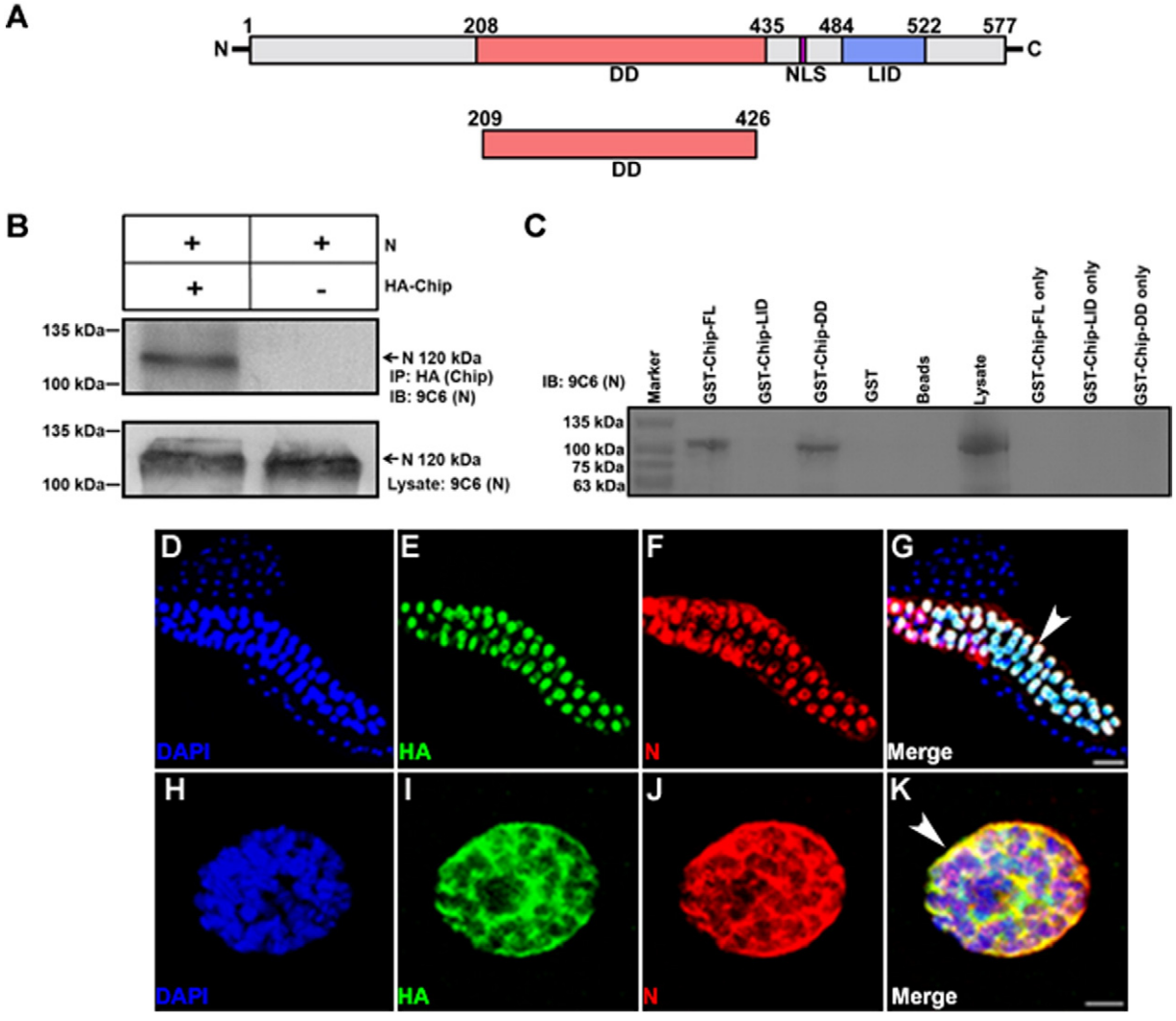

Fig. 1. Interaction between the Chip and Notch proteins. (A) Schematic representation of the domain organization of Chip. Different domains of Chip are marked at the bottom, while the boundary residues are marked on the top. Dimerization domain (DD); nuclear localization signal (NLS); LIM interaction domain (LID) (see refs. [27,28]). Based on yeast two-hybrid analysis, a region of Chip (amino acids 209–426) that was sufficient for binding to Notch is shown below the full-length protein. (B) Co-immunoprecipitation of HA-Chip and Notch-ICD: HA-Chip and Notch-ICD proteins were co-expressed in larval salivary glands and immunoprecipitated with anti-HA agarose. Immunoprecipitated proteins were analyzed by Western blotting with anti-Notch (C17.9C6) antibodies (upper panel). Lower panel shows the level of Notch protein in the lysates. (C) GST pull-down assay was performed with lysate of salivary glands in which Notch-ICD was overexpressed using *sgs-GAL4* driver and purified recombinant GST-Chip full-length (amino acids 1–577), Chip-DD (amino acids 208–435), Chip-LID (amino acids 436–577), and other controls as indicated. GST pulled-down proteins were analyzed by Western blotting with anti-Notch (C17.9C6) antibodies. Note that GST-Chip full-length and GST-Chip-DD pulled down Notch-ICD. (D–K) Co-localization of HA-Chip and Notch-ICD in salivary glands: *UAS-HA-Chip* and *UAS-Notch-ICD* were expressed under the control of the *sgs-GAL4* driver. Images presented in figures H–K are high-magnification images of a single cell from salivary glands as shown in figures D–G. Images in G and K are merges of those in D–F and H–J, respectively. Co-expression of HA-Chip and Notch-ICD shows their co-localization in cell nuclei (arrowheads). Scale bars, 100 μm (D–G), 10 μm (H–K).

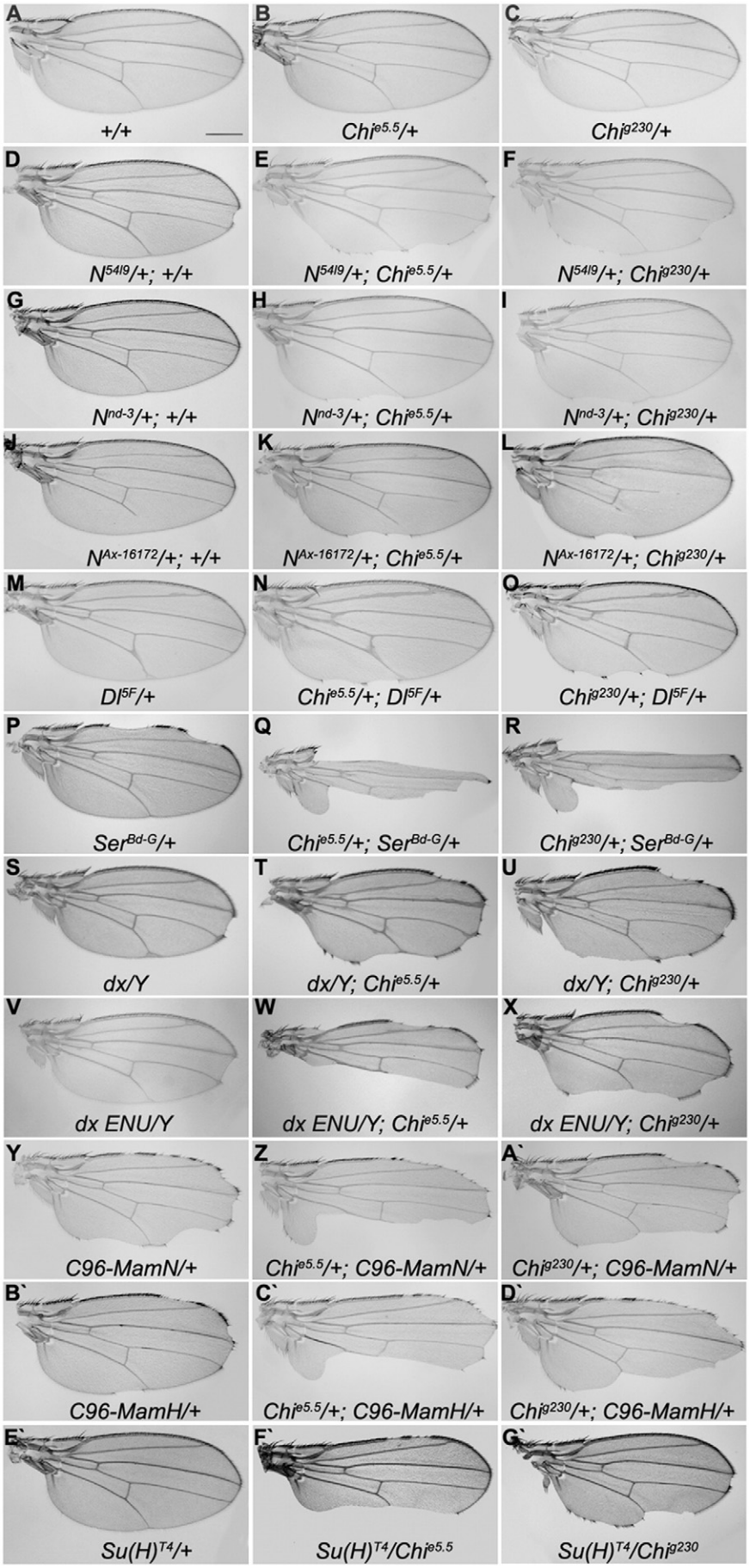
A
+/+
B
Chi^e5.5/+
C
Chi^g230/+
D
N^54l9/+; +/+
E
N^54l9/+; Chi^e5.5/+
F
N^54l9/+; Chi^g230/+
G
N^nd-3/+; +/+
H
N^nd-3/+; Chi^e5.5/+
I
N^nd-3/+; Chi^g230/+
J
N^Ax-16172/+; +/+
K
N^Ax-16172/+; Chi^e5.5/+
L
N^Ax-16172/+; Chi^g230/+
M
Dl^5F/+
N
Chi^e5.5/+; Dl^5F/+
O
Chi^g230/+; Dl^5F/+
P
Ser^Bd-G/+
Q
Chi^e5.5/+; Ser^Bd-G/+
R
Chi^g230/+; Ser^Bd-G/+
S
dx/Y
T
dx/Y; Chi^e5.5/+
U
dx/Y; Chi^g230/+
V
dx ENU/Y
W
dx ENU/Y; Chi^e5.5/+
X
dx ENU/Y; Chi^g230/+
Y
C96-MamN/+
Z
Chi^e5.5/+; C96-MamN/+
A`
Chi^g230/+; C96-MamN/+
B`
C96-MamH/+
C`
Chi^e5.5/+; C96-MamH/+
D`
Chi^g230/+; C96-MamH/+
E`
Su(H)^T4/+
F`
Su(H)^T4/Chi^e5.5
G`
Su(H)^T4/Chi^g230

and Chip form a functional complex, which is a tetramer formed by two Ap molecules bridged by two Chip molecules, was established [25,27,28,30]. Chip has also been reported for regulating axon guidance [31], posteclosion behavior [32], and establishing the boundary of the eye field [33] in *Drosophila*.

In the early wing primordium, Ap induces expression of Fringe and Notch ligand Serrate (Ser) in dorsal cells and another Notch ligand Delta (Dl) in the ventral cells [34–36]. Ser in dorsal cells and Dl in ventral cells activate Notch symmetrically in cells on either side of the DV compartment boundary [34,37–39]. The glycosyltransferase Fringe modifies Notch in dorsal cells that makes Notch more sensitive to Dl and less sensitive to Ser [40–42]. Activation of Notch results in Wingless (Wg) expression in cells along the DV boundary. Subsequently, in the third instar larval wing disc, Ap induces expression of Beadex/dLMO, which negatively regulates Ap activity [29,43,44]. Beadex/dLMO encodes a LIM-only type protein containing two LIM domains. It has been found that dLMO binds to Chip more efficiently and competes with Ap for binding to Chip, thereby inactivating Ap [28,30,43]. At this stage, when Ap is inactivated, Notch signaling in the DV boundary remains maintained by the establishment of a positive feedback loop between Wg-expressing cells along the DV boundary and Ser and Dl-expressing cells in adjacent dorsal and ventral cells, respectively. Ser and Dl continue to activate Notch and, as a result, Wg and Cut expressions remain maintained along the DV boundary.

Using molecular and genetic analyses, we found that the correct amount of Chip and Notch is critical at the DV boundary for wing margin formation and that Notch function in DV boundary formation is mediated by the Notch–Chip heterodimer. In addition, we have also detected that excess Chip rescues Notch-induced proliferation effects.

2. Materials and methods

2.1. Yeast two-hybrid

A 642 bp *Drosophila* Notch cDNA (accession number M11664) fragment, which encodes amino acids 1896–2109, was amplified by polymerase chain reaction (PCR) and cloned in-frame with the sequence encoding the LexA DNA-binding domain of bait vector. This construct was used as bait to screen oligo (dT)-primed *D. melanogaster* 0–24 h embryo cDNA libraries cloned in pGAD prey vectors containing GAL4 activation domains. A yeast two-hybrid screen was performed as described previously [19]. His + colonies were selected on media lacking tryptophan, leucine, and histidine. All positive pGAD plasmids from His + colonies were isolated and sequenced to identify interactors.

2.2. Immunoprecipitation, GST pull-down, and immunoblotting

For immunoprecipitation, Notch-ICD and HA-Chip proteins were expressed in larval salivary glands under the control of *sgs-GAL4* driver. Salivary glands were lysed in lysis buffer containing 25 mM Tris, pH 8.0, 27.5 mM NaCl, 20 mM KCl, 25 mM sucrose, 10 mM EDTA, 10 mM EGTA, 1 mM DTT, 10% glycerol, 0.5% Tergitol solution, 1 mM PMSF, and complete protease inhibitor (Roche), lysates were cleared by centrifugation at 12,000 rpm for 20 min and incubated with anti-HA affinity beads (Sigma) for 3 h. After washing with lysis buffer thrice, protein complexes were eluted with SDS sample buffer, separated on SDS protein gels, transferred onto PVDF membrane (Bio-Rad), and finally, probed with monoclonal mouse anti-Notch (C17.9C6) antibody at 1:3000 and mouse anti-HA antibody at 1:1000 dilution (Sigma).

For GST pull-down, DNA fragments coding for full-length Chip (amino acids 1–577), N-terminal Chip-DD (amino acids 208–435), and C-terminal Chip-LID (amino acids 436–577) were cloned into pGEX-4T-1 vector (Amersham). The following forward and reverse primers were used for PCR amplification of different fragments of *Chip* (GenBank accession number AY058561):

Full-length *Chip*—5′CGCAGGAATTCATGAATCGTAGGGGTTTG3′ and 5′GCGAGGCGGCCGCCTATTGCGATACAATGG3′,
N-terminal *Chip-DD*—5′CGCAGGAATTCCGGCACAATTCCTACTTTAGC 3′ and 5′GCGAGGCGGCCGCGGGCGGAGCCACCATGC3′,
and C-terminal *Chip-LID*—5′CGCAGGAATTCGGCAAGAAGGATCCGC3′ and 5′GCGAGGCGGCCGCCTATTGCGATACAATGG3′ primers.

Intact reading frames for all constructs were verified by DNA sequence analysis. GST and GST fusion proteins were expressed in *E. coli* BL21 cells at 37 °C with 2 mM isopropyl-1-thio-β-D-galactopyranoside (IPTG) induction. Bacteria were lysed in a solution of Cell Lytic™ express tablet (Sigma) with complete protease inhibitor (Roche). Glutathione Sepharose (GE Healthcare Bio-Sciences) beads were washed in cold phosphate-buffered saline (PBS) three times for 30 min each; a 50% slurry was made in PBS.

The intracellular domain of Notch was overexpressed in salivary glands by salivary gland–specific GAL4 driver (*sgs-GAL4*), and the third instar larval salivary glands were dissected and washed in PBS, then lysed in lysis buffer (50 mM Tris pH 8.0, 0.1% TritonX-100, 10% Glycerol, 200 μg/ml lysozyme, and 1 mM PMSF) for 3 h at 4 °C. The supernatant was collected after centrifugation for 20 min at 12,000 rpm.

Glutathione sepharose beads alone or incubated with GST fusion proteins mixed with salivary gland lysate and rotated for 3 h at 4 °C followed by washing with PBST (1× PBS, 1% Triton-X-100) thrice, 15 min each. Beads were boiled in 2× Laemmli buffer for 5 min, and the samples were loaded in 12% denaturing gel with Spectra Multicolor Broad Range Protein Ladder used as a marker (Fermentas). Proteins were separated on non-reducing SDS-PAGE (without β-mercaptoethanol) and transferred onto PVDF membrane (Bio-Rad). Blot was probed with mouse anti-Notch C17.9C6 in 1:3000 dilution (Developmental Studies Hybridoma Bank) and secondary antibody goat anti-mouse IgG-AP conjugate in 1:2000 dilution (Molecular Probes) in blocking solution (4% skimmed milk in TBST—50 mM Tris, pH 7.5, 150 mM NaCl, 0.1% Tween-20). Then, after washing in TBST thrice, color was detected by Sigma FAST™ BCIP/NBT (Sigma).

2.3. Drosophila genetics

All fly stocks were maintained on standard cornmeal/yeast/molasses/agar medium at 25 °C. The $Chi^{e5.5}$/*CyO* and $Chip^{g230}$/*CyO* stocks were obtained from Bloomington Drosophila Stock Center (Bloomington, IN). *UAS-ChipΔDD* and *UAS-ChipΔLID* stocks were obtained from Donald J. van Meyel. We used the following alleles of Notch pathway components for genetic interaction studies: N^{54l9}, $N^{md\text{-}3}$, $N^{Ax\text{-}16172}$, Dl^{5F},

Fig. 2. Genetic interactions of *Chip* mutants with Notch pathway components. (A–G`) Representative wings from individuals with indicated genotypes are shown. Wings from wild-type individuals (A) and *Chip* heterozygotes (B and C) showed normal wing phenotype. Wings from N^{54l9} heterozygotes (D) showed the wing nicking phenotype, which was enhanced in transheterozygous combination with *Chip* alleles (E and F). Wings from females heterozygous for $N^{md\text{-}3}$ showed normal wing phenotype (G), whereas in transheterozygous combinations with *Chip* alleles, it displayed a wing margin nicking phenotype (H and I). Gain-of-function N allele $N^{Ax\text{-}16172}$ (J) displayed shortened longitudinal vein L5, which in transheterozygous combination with different alleles of *Chip* showed shortening of both L4 and L5 along with occasional wing nicking phenotype (K and L). Heterozygotes of Notch ligand *Delta* (Dl^{5F}) displayed wing vein thickening phenotype (M), whereas in transheterozygous combinations with *Chip* alleles, it showed stronger wing vein thickening as well as wing nicking phenotype (N and O). Wing notching phenotype of $Ser^{Bd\text{-}G}$ (P) was severely enhanced in transheterozygous combinations with different alleles of *Chip* (Q and R). Hemizygotes of *dx* alleles, *dx* and dx^{ENU} showed vein thickening in the distal region and sporadic wing nicking (S and V), which were enhanced by reducing the dose of *Chip* (T and U, W and X). Dominant-negative *Mastermind*, *MamH*, and *MamN* in heterozygous condition displayed wing notching phenotype (Y and B`), which was enhanced in transheterozygous combinations with *Chip* (Z and A`, C` and D`). Gain-of-function mutant allele of suppressor of hairless, $Su(H)^{T4}$, showed normal wing phenotype in heterozygous condition (E`), which in transheterozygous combinations with *Chip* alleles showed significant wing nicking phenotype (F` and G`). Scale bar, 250 μm.

Ser$^{Bd\text{-}G}$, *MamH*, *MamN*, *Su(H)*^{T4}, *ec dx*, and *dx*^{ENU}. To generate somatic clones using the FLP/FRT system, *FRT42B Chip*$^{e5.5}$*/CyO* stock was constructed from *Chi*$^{e5.5}$*/CyO* and *FRT42B* stocks by appropriate genetic crosses. To generate somatic clones in wing imaginal discs, females of *y w hsFLP; Ubi-GFP FRT42B* were crossed to male *FRT42B Chip*$^{e5.5}$*/CyO* flies. Heat shock was given at 37 °C for 45 min at 24 h after egg laying (AEL), and the third instar larvae were analyzed for mutant clones. For generating the *P[UAS–HA–Chip]*, a full-length *Chip* cDNA with a HA tag at the amino-terminus was cloned in the pUAST vector. This construct was introduced into *w*^{1118} embryos by germline transformation following the standard procedures. Multiple independent insertions were obtained. The UAS constructs were expressed under the control of *sgs-GAL4*, *en-GAL4*, *ptc-GAL4*, *C96-GAL4*, and *ap-GAL4* drivers. To co-express different domains of Chip along with Notch-ICD, *w; UAS-HA-Chip/CyO; UAS-Notch-ICD/TM6B, w; UAS-Notch-ICD/CyO; UAS-ChipΔDD/TM6B*, and *w; UAS-Notch-ICD/CyO; UAS-ChipΔLID/TM6B* stocks were generated by appropriate genetic crosses.

2.4. Immunocytochemistry and confocal microscopy

Drosophila third instar larval imaginal discs and salivary glands were dissected in cold PBS. Immunostaining of these tissues was performed as described previously [19]. Primary antibodies (rabbit anti-HA at 1:100 dilution (Sigma), mouse anti-Notch (C17.9C6) at 1:300 dilution, mouse anti-Wg (4D4), rat anti-Elav at 1:200, mouse anti-Cut (2B10) at 1:100 (Developmental Studies Hybridoma Bank), and rabbit anti-PH3 at 1:500 (Millipore)) and secondary antibodies (sheep anti-mouse antibodies conjugated to Cy3 at a 1:200 dilution (Sigma), goat anti-rat antibodies conjugated to FITC at a 1:200 dilution (Sigma), goat anti-rabbit antibodies Alexa Flour 555 at a 1:200 dilution (Invitrogen), and goat anti-rabbit antibodies conjugated to FITC at a 1:200 dilution (Jackson ImmunoResearch Laboratories, West Grove, PA)) were used for immunostaining. After washing secondary antibodies, DAPI (4′, 6-diamidino-2-phenylindole dihydrochloride) was used to detect the nucleus and washed twice in PBS for 10 min each. Then, larval tissues were mounted in FluoroGuard Antifade Reagent (Bio-Rad), and the images were captured with a Zeiss LSM510 Meta laser confocal microscope.

2.5. Quantitative RT-PCR

Quantitative real-time PCR was carried out as per the manufacturer's protocol (Applied Biosystem). A total of 20 μl of the reaction volume included 10 μl 2× SYBR green, 0.25 μl each forward and reverse primer, and 1 μl cDNA, and PCR was performed using ABI 7500 instrument. Reaction conditions were as follows: an initial incubation at 50 °C for 2 min followed by denaturation for 10 min at 95 °C and 40 cycles at 95 °C for 15 s and 60 °C for 1 min. Data were normalized to *rps17* before calculating the fold change. Changes in gene expression were calculated using the $2^{-\Delta\Delta CT}$ method.

2.6. Cell counting

Eye-antennal discs, where *UAS-Notch-ICD* and both *UAS-HA-Chip/CyO* and *UAS-Notch-ICD* were overexpressed by *ey-GAL4* and *ey-GAL4/+* discs, were dissected from the third instar larvae in Grace's Insect Media. To determine the number of cells in each disc of different genotypes, a single-cell suspension of eye-antennal discs was prepared in 1 mg/ml collagenase (Sigma). Cells were counted using Neubauer hemocytometer under a light microscope.

3. Results

3.1. Notch physically interacts with Chip

In an effort to identify novel components involved in Notch signaling pathway, a yeast two-hybrid screen was performed using the portion of intracellular domain of Notch receptor as bait, and we identified *Drosophila* Chip as an interacting partner of Notch. The yeast two-hybrid screen of 6×10^6 cDNAs from a *Drosophila* 0–24 h embryonic library was carried out using Ankyrin repeat region of Notch-ICD (amino acids 1896–2109) as bait. Five positive clones (His$^+$) were isolated and found to encode overlapping *Chip* cDNAs. Sequence analysis of these clones revealed that the dimerization domain of Chip (amino acids 209–426) is necessary and sufficient for binding Notch-ICD (Fig. 1A). This particular domain of Chip was earlier shown to interact with the dimerization domain of another molecule of Chip, and the resultant Chip dimer is required to bridge two Ap molecules to form a functional tetrameric complex for Ap-mediated gene transcription [25,27,28,30].

Co-immunoprecipitation experiments confirmed the interaction between Notch and Chip. Notch protein was immunoprecipitated with HA-Chip protein from larval salivary glands when both Notch-ICD and HA-Chip were co-expressed (Fig. 1B). Furthermore, GST pull-down experiments using purified GST-Chip confirmed the interaction between Notch and Chip. Deletion analysis of Chip protein showed that N-terminal Chip-DD is required for binding to Notch-ICD (Fig. 1C). To extend the analysis of the interaction between Chip and Notch, we further investigated the subcellular localization of these proteins when *UAS-HA-Chip* and *UAS-Notch-ICD* were co-expressed in larval salivary glands using *sgs-GAL4* driver. Immunocytochemical analysis revealed that Chip and Notch-ICD indeed co-localized in cell nuclei (Fig. 1D–K).

3.2. Chip interacts genetically with Notch pathway components

To address the functional implications of the physical interaction between the Chip and Notch proteins, we tested whether mutations in *Chip* and *Notch* pathway components display genetic interactions in transheterozygous combinations. We used two independent loss-of-function *Chip* alleles: *Chip*$^{e5.5}$ and *Chip*^{g230} [26]. *Chip*$^{e5.5}$ is a null mutation, which is basically a small deletion that shifts the reading frame, while *Chip*^{g230} [*Df(2R)Chip*^{g230}] is a deficiency line that deletes *Chip* [26,45]. Flies, heterozygous for either *Chip*$^{e5.5}$ or *Chip*^{g230}, have normal wings (see ref. [26]; Fig. 2A–C). Female flies heterozygous for *Notch* null allele, *N*^{54l9}, have a weakly-penetrant wing-nicking phenotype (Fig. 2D) and a transheterozygous combination of *N*^{54l9} and one of the two *Chip* null alleles resulted in enhancement of wing nicking phenotype, indicating further reduction of the Notch function (Fig. 2E and F). Female flies heterozygous for *Notch* hypomorphic allele, *N*$^{nd\text{-}3}$, do not display any wing-nicking phenotype (Fig. 2G), whereas they display wing margin defects (Fig. 2H and I) in transheterozygous combinations with *Chip* alleles. Gain-of-function *Notch* allele, the *Abruptex* mutation (*N*$^{Ax\text{-}16172}$), which displays a shortened longitudinal vein V (L5), also exhibited occasional wing nicking phenotype as well as L4 and L5 wing-vein shortening in transheterozygous combination with *Chip* mutations (Fig. 2J–L). The *Notch* ligand *Delta* (*Dl*^{5F}) heterozygotes display only wing vein thickening phenotype; however, removing one copy of *Chip* resulted in wing vein thickening as well as moderate wing notching in the posterior side (Fig. 2M–O). The wing notching phenotype of the dominant negative mutation of *Serrate* (*Ser*$^{Bd\text{-}G}$) was also severely enhanced by reducing the dose of *Chip* (Fig. 2P–R). Flies hemizygous for *dx*, a cytoplasmic modulator of Notch activity, display distal wing vein thickening with occasional wing notching (Fig. 2S) and this phenotype was strongly enhanced by removing one copy of *Chip* (Fig. 2T and U). Another *dx* allele, *dx*^{ENU}, also showed similar phenotype (Fig. 2V–X). *MamN* and *MamH* are C-terminal truncations of transcriptional co-activator *Mastermind* (*Mam*) gene [46]. *C96-GAL4*-driven expression of dominant-negative, C-terminal Mam truncations in *C96-GAL4, UAS-MamN* and *C96-GAL4*, *UAS-MamH* lines (*C96-MamN* and *C96-MamH*) display fully penetrant wing-nicking phenotype [46,47] (Fig. 2Y and B`). Reducing the dose of *Chip* in *C96-MamN/+* or *C96-MamH/+* individuals elicited enhanced wing notching phenotype

(Fig. 2Z and A`, and C` and D`). The wing notching phenotype of gain-of-function allele of suppressor of hairless, $Su(H)^{T4}$, was also enhanced by removing a copy of *Chip* (Fig. 2E`-G`). Our study demonstrated that *Chip* and *Notch* pathway components show very strong genetic interactions.

3.3. Chip mutant clones in the dorsal compartment of the wing discs express Notch and its targets, Wg and Cut, for inducing ectopic wing margin

To further investigate the molecular implications of Chip and Notch interaction *in vivo*, we examined the effects of *Chip* loss-of-function on

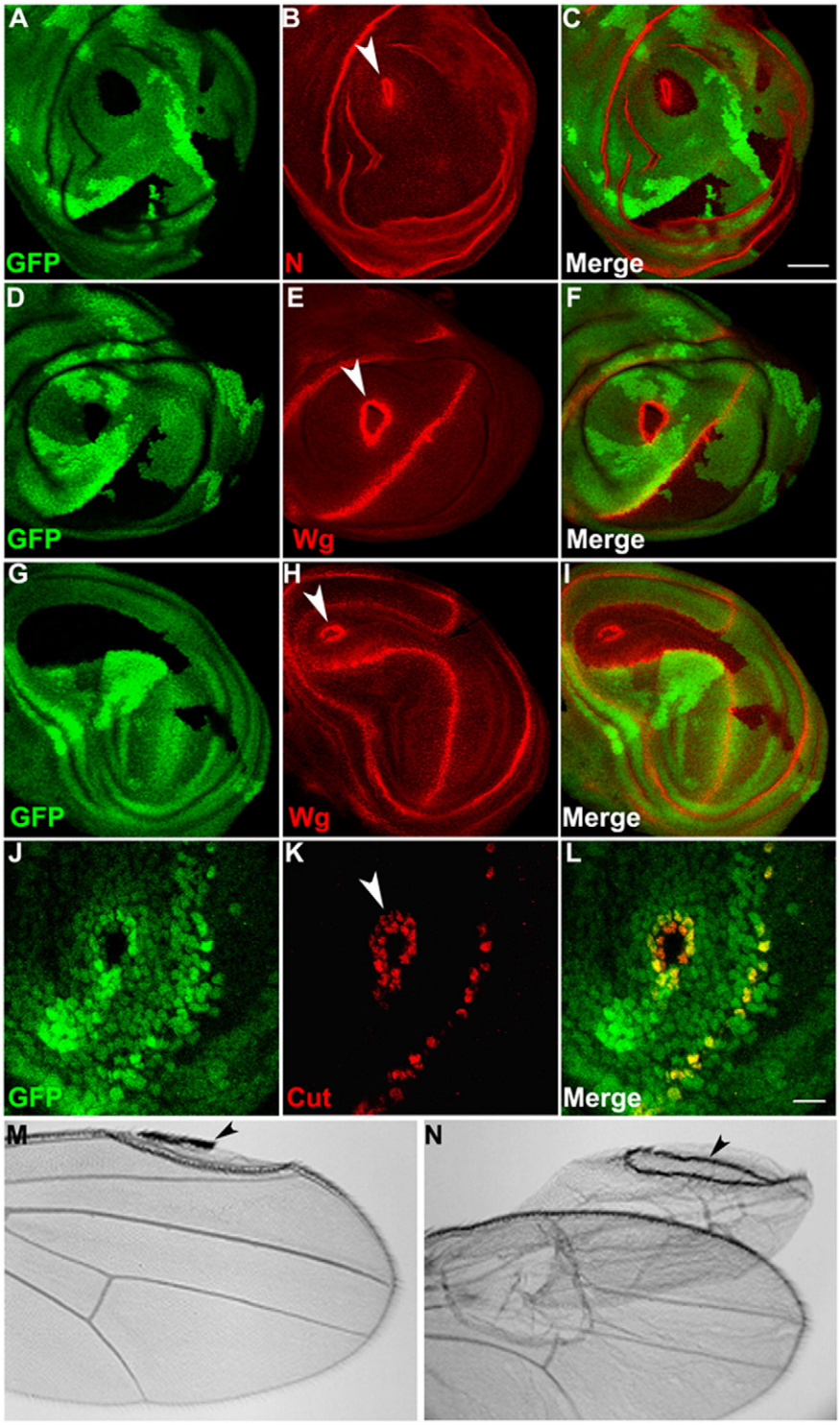

Fig. 3. Loss of *Chip* function in the dorsal compartment of the wing discs results in ectopic expression of Notch and its targets and induces ectopic wing margins. (A–L) *Chip* loss-of-function clones in the third instar larval wing imaginal discs: *Chip* mutant clones in the dorsal compartment only show ectopic expression of Notch (A–C), Wg (D–F and G–I), and Cut (J–L) (arrowheads). Note that *Chip* mutant clones, which did not respect the DV boundary (G–I), displaced Wg expressing DV stripe around the clone (arrow) and showed ectopic Wg expression only in the dorsal compartment (arrowhead). *Chip* mutant clones in adult wings showed wing outgrowths and ectopic wing margins (M–N) (arrowheads). Images presented in C, F, I, and L are merged images of those presented in A and B, D and E, G and H, and J and K, respectively. Scale bars for A–I, 50 μm and J–L, 5 μm.

the endogenous Notch protein and its targets, Wg and Cut. We generated *Chip* loss-of-function clones in larval wing imaginal discs, using a $Chip^{e5.5}$ null mutant [26] and the FLP/FRT system [48]. The FLP activity, which is under the control of *hsp70* promoter (*hs-FLP*), was used to induce somatic recombination events in wing discs, and the *Chip* mutant clones were identified by the absence of GFP expression.

$Chip^{e5.5}$ mutant somatic clones in the ventral compartment of the wing discs showed no ectopic expression of Notch or its targets (Wg and Cut). In contrast, *Chip* mutant clones located in the dorsal compartment showed ectopic expression of Notch and its targets (Wg and Cut) (Fig. 3A–L). *Chip* mutant clones, which did not respect the DV boundary, also showed ectopic Wg expression only in the dorsal compartment and they displaced the Wg expressing stripe around the clone (Fig. 3G–I). *Chip* mutant clones in the dorsal compartment of the wing disc resulted in wing outgrowth and ectopic wing margin formation (Fig. 3M and N). Earlier, it was shown that *Chip* clones generated in the ventral compartment of the wing disc had no effect, whereas clones in the dorsal compartment of the disc were associated with wing outgrowths and ectopic wing margins [25]. It has also been reported that cells within *Chip* mutant clones in the dorsal compartment of the wing disc change their identity and become ventral cells, while normal cells, neighboring these mutant clones, were induced to form the ectopic wing margin [25]. In the present study, we clearly found that the border cells of *Chip* mutant clones started expressing ectopically Notch and its downstream targets (Wg and Cut), which is responsible for making DV boundary adjoining the mutant clones and formation of the ectopic wing margins (Fig. 3). These results strengthened the view that both Notch and Chip play important roles in wing margin formation.

3.4. Overexpression of Chip causes similar phenotypes as Notch loss-of-function in DV boundary of wing disc

To examine whether overexpression of *Chip* influences the expression of Notch and its targets (Wg and Cut) and consequently, wing margin formation, we overexpressed *Chip* in different domains of wing discs using the GAL4/UAS system [49]. Overexpression of Chip in the posterior compartment of the wing discs using *engrailed-GAL4* (*en-GAL4*) driver resulted in significant reduction of Wg and Cut expression along the DV boundary exclusively in *en-GAL4* expressing posterior compartment (Fig. 4A–H). As a consequence, a massive cut of the posterior wing margin was clearly visible in adult wings (Fig. 4M). When we expressed Chip using *patched-GAL4* (*ptc-GAL4*) driver, we noticed complete loss of Cut expression in patched domain of DV margin of wing discs (Fig. 4N–Q); consequently, a nick in the adult wing margin, exactly in the patched domain, became visible (Fig. 4R). Interestingly, Notch expression and its distribution remained unaffected in *en-GAL4*–driven Chip overexpressing cells (Fig. 4I–L). These observations suggest that although Notch expression is normal in the DV margin in these wing discs, it cannot be functional in this particular region due to the presence

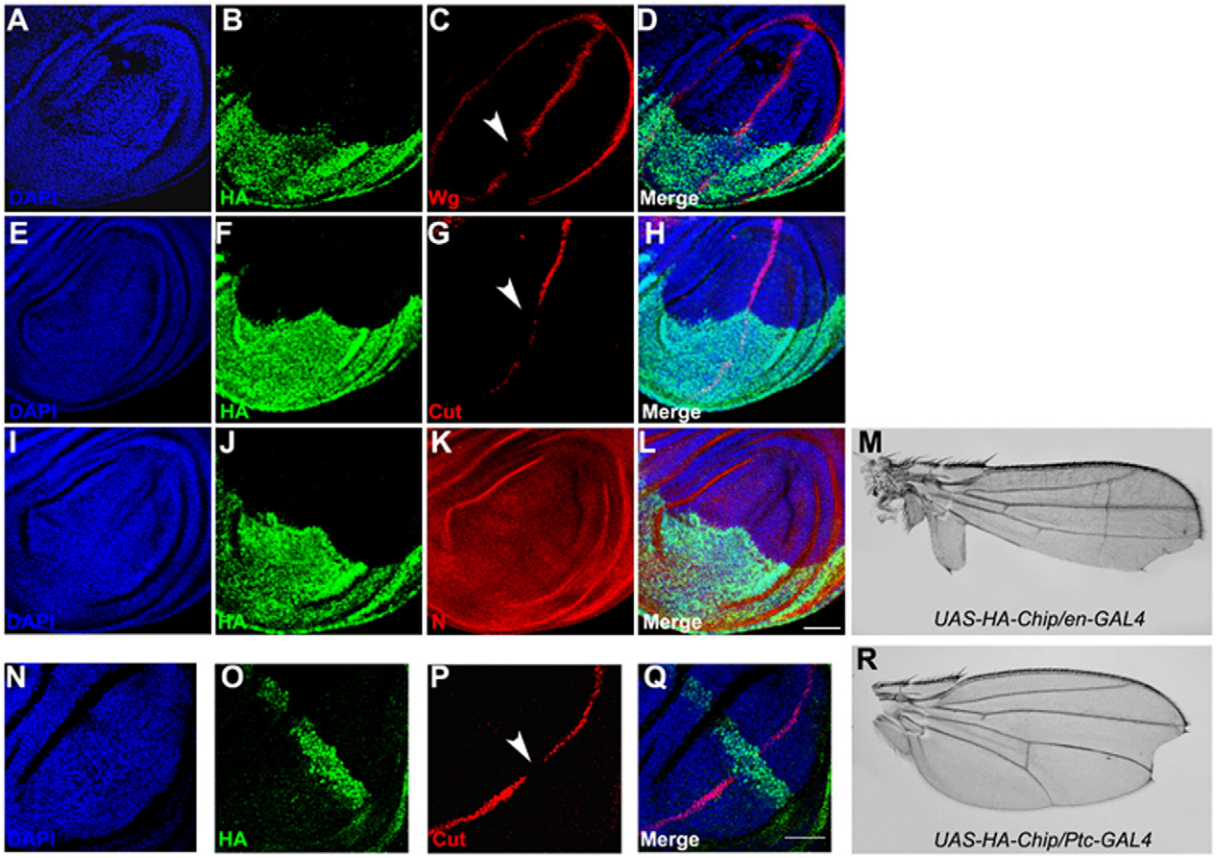

Fig. 4. Overexpression of *Chip* causing Notch loss-of-function phenotypes without altering the expression and distribution of Notch protein. Overexpression of *Chip* in the posterior compartment of wing discs with *en-GAL4* driver (A–L) and in anterior–posterior compartment boundary of wing disc with *ptc-GAL4* driver (N–Q). Note that overexpression of *Chip* using *en-GAL4* driver showed significant reduction in Wg (A–D) and Cut (E–H) expressions (shown by arrowheads); however, expression and distribution of Notch protein (I–L) remains unaltered in the *en-GAL4* expressing posterior compartment of the disc. Adult flies, in which Chip was overexpressed using *en-GAL4* driver, also showed massive notching in the posterior wing margin (M). Similarly, *ptc-GAL4*–driven Chip overexpression showed complete loss of Cut expression in the patched domain of DV margin of wing imaginal discs (N–Q) (arrowhead). A nick in the adult wing margin exactly in the patched domain was clearly visible (R). Images in D, H, L, and Q are merges of those in A–C, E–G, I–K, and N–P, respectively. Scale bars for A–L and N–Q, 50 μm.

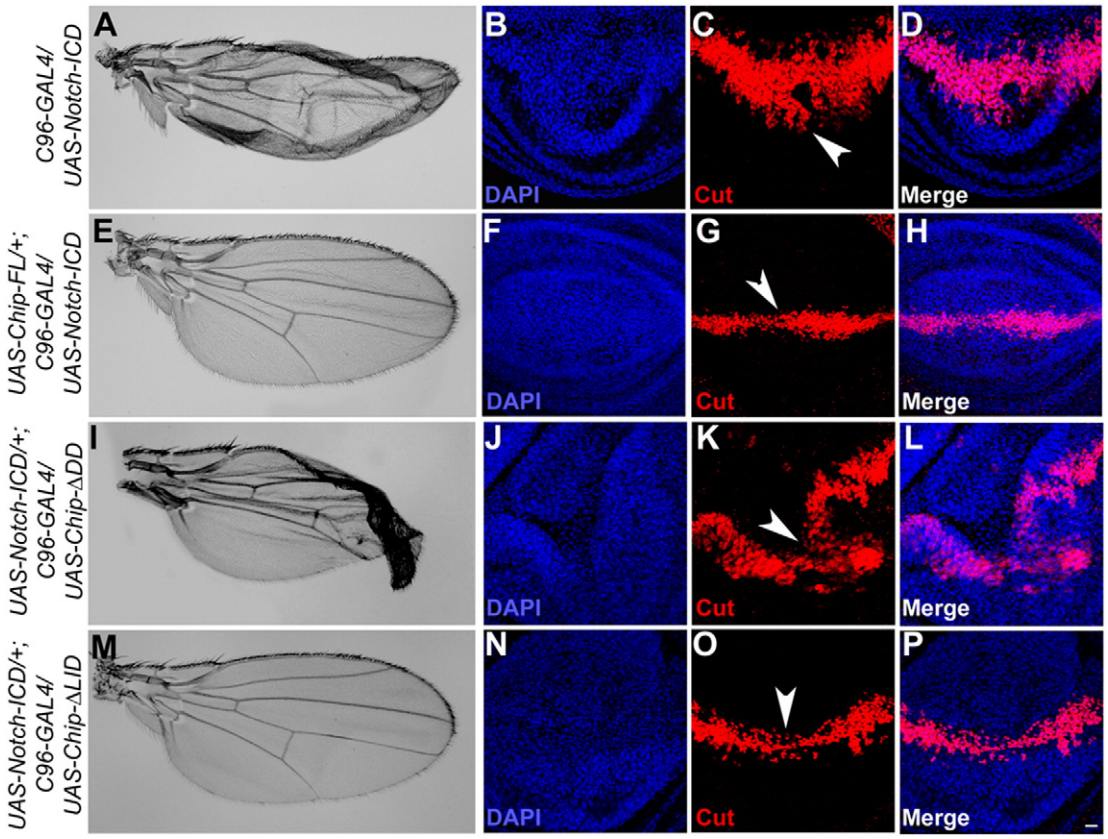

Fig. 5. Chip overexpression significantly rescues the phenotype caused by excess Notch activity in the wing margin. *UAS-Notch-ICD* (A–D), *UAS-Chip-FL* and *UAS-Notch-ICD* (E–H), *UAS-Chip-ΔDD*, and *UAS-Notch-ICD* (I–L), *UAS-Chip-ΔLID* and *UAS-Notch-ICD* (M-P) transgenes were overexpressed under the control of *C96-GAL4* driver, which is expressed in cells corresponding to the DV boundary of the wing imaginal discs. Endogenous Cut levels were monitored with the Cut (2B10) antibody. Expression of Notch-ICD alone resulted in massive wing margin defects (A), and Cut expressing domain was also broadened (B–D) (arrowhead). (E–H) Coexpression of both Chip full-length and Notch-ICD resulted in significant rescue of wing margin defects (E), and Cut expression was also almost normal in DV boundary (F–H) (arrowhead), (I–L) Coexpression of Chip-ΔDD and Notch-ICD did not show any rescue of wing margin defects (I), and Cut expression was also remain broadened in DV boundary (J–L) (arrowhead), (M–P) coexpression of Chip-ΔLID and Notch-ICD led to significant rescue of wing margin defects (M), and Cut expression was also almost normal in DV boundary (N–P) (arrowhead). Images presented in D, H, L, and P are merges of those in B and C, F and G, J and K, and N and O, respectively. Scale bars, 10 μm (B–D, F–H, J–L, N–P).

of an excess amount of Chip. Thus, it is evident that the relative amounts of Notch and Chip are critical for normal DV margin formation. Here, we should mention that these results do not rule out the possibility of the involvement of excess Chip on altering Ap activity and consequently reducing the expression of Notch ligand Serrate, which resulted in loss of Notch activity.

3.5. Chip overexpression significantly rescues the phenotypes caused by excess Notch

We noticed that overexpression of *Chip* can rescue the phenotype caused by excess Notch activity in the wing margin (Fig. 5). As Notch binds to dimerization domain of Chip, we also examined which domain

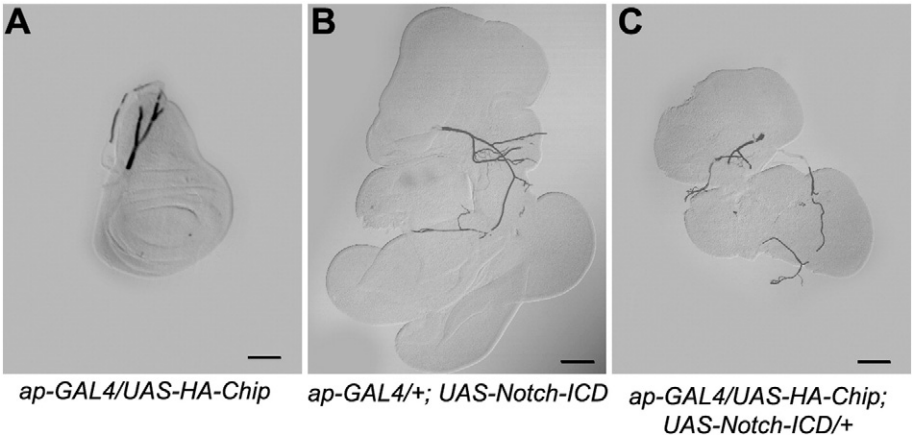

Fig. 6. Phenotypes caused by excess Notch activity in wing imaginal discs can significantly be rescued by simultaneous overexpression of Chip. Wing imaginal discs, where *UAS-HA-Chip* (A), *UAS-Notch-ICD* (B), and both *UAS-HA-Chip* and *UAS-Notch-ICD* (C) were overexpressed by *ap-GAL4*, showed notably reduced size of tumorous wing disc in which both *Notch-ICD* and *Chip* were overexpressed (C), compared to only *Notch-ICD* overexpressing wing disc (B). Scale bars for A, B, and C, 100 μm.

of Chip can rescue the Notch gain-of-function phenotype in wing discs. We simultaneously overexpressed full-length *Chip* or *Chip-ΔDD*, or *Chip-ΔLID* along with *Notch-ICD* in the presumptive wing margin using a wing margin–specific GAL4 line, *C96-GAL4*. Full-length *Chip* and *Chip-ΔLID* significantly rescued the wing margin defects caused by overexpression of *Notch-ICD*, whereas *Chip-ΔDD* could not rescue this phenotype (Fig. 5A, E, I, M). Similarly, we noticed that overexpression of full-length *Chip* or *Chip-ΔLID* with *Notch-ICD* in the DV boundary area, using *C96-GAL4* driver, restored the almost normal Cut expression, which was found to be significantly broadened in *C96-GAL4* expressing domain in the DV boundary of wing discs from individuals overexpressing only *Notch-ICD* (Fig. 5B–D, F–H, N–P). However, Cut expression was not reinstated when *Notch-ICD* and *Chip-ΔDD* were overexpressed simultaneously (Fig. 5J–L).

Earlier, it had been shown that overexpression of the activated form of Notch in wing discs resulted in the hyperproliferation of the disc [50]. We have also observed that overexpression of *Notch-ICD* using *ap-GAL4* driver exhibited tumorous phenotype of the wing discs (Fig. 6A and B) and this phenotype was reduced by simultaneous overexpression of *Chip* (Fig. 6C). Similarly, the eye disc, where both *Notch-ICD* and *Chip* were co-overexpressed, showed reduced size as well as less disorganized and fused ommatidia compared to only *Notch-ICD* overexpressing in eye discs (Fig. 7A–O). Moreover, each eye disc, where both *Notch-ICD* and *Chip* were co-overexpressed, contained a fewer number of cells compared to the disc in which only *Notch-ICD* was overexpressed (Fig. 7P). In order to determine the level of expression of a few Notch target genes, such as *deadpan*, *dMyc*, *string/cdc25* and tumor suppressor gene *p53* in only *Notch-ICD* or both *Notch-ICD* and *Chip* expressing eye discs, quantitative real-time PCR was carried out and we found that expression levels of *p53* and *dMyc* were upregulated, while that of *deadpan* and *string/cdc25* were downregulated in both *Notch-ICD* and *Chip* expressing discs compared to only *Notch-ICD* expressing discs (Fig. 7Q).

While examining the only *Notch-ICD* or both *Notch-ICD* and *Chip* overexpressing eye discs using anti-phospho-Histone H3 (PH3)

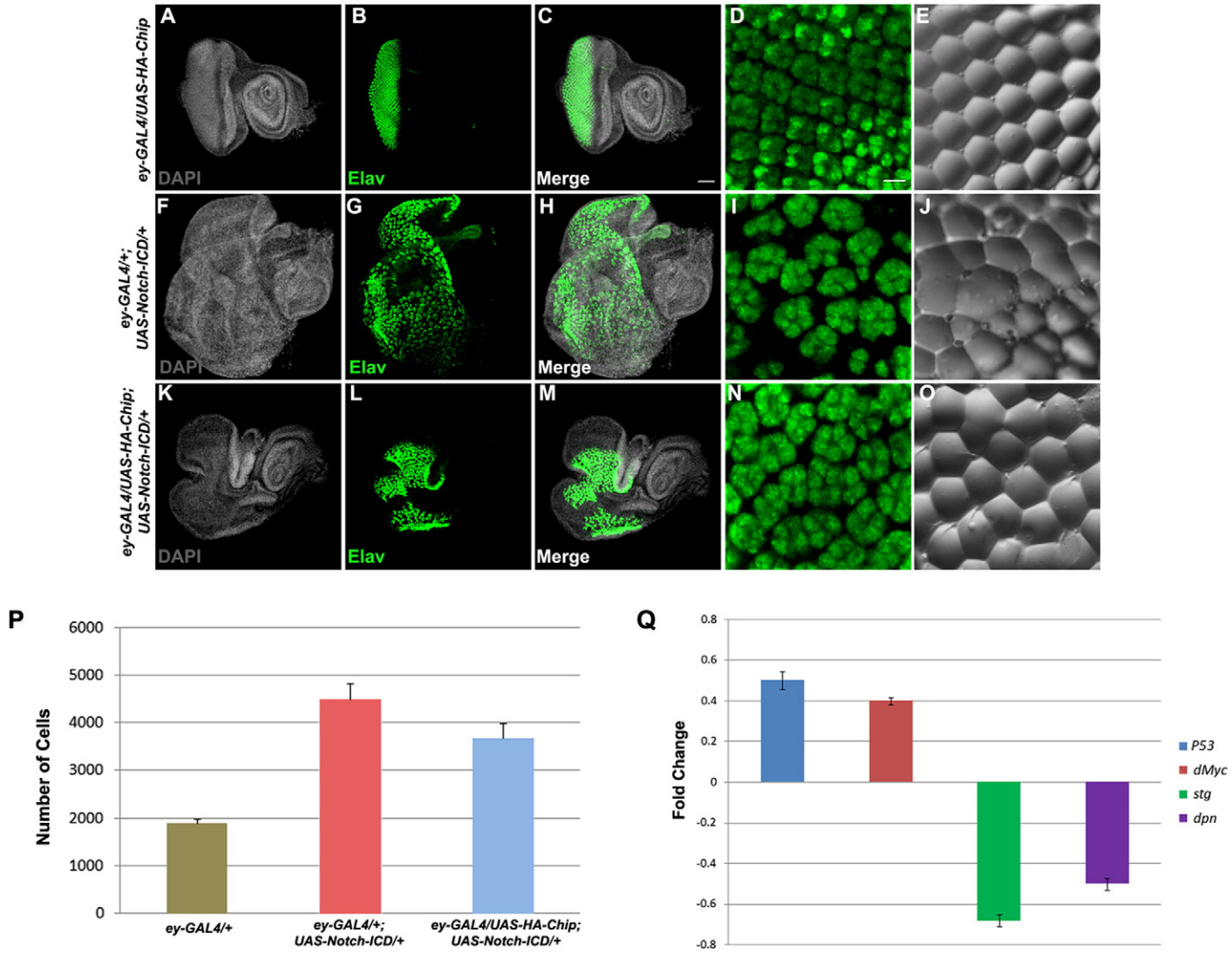

Fig. 7. Phenotypes caused by excess Notch activity can significantly be rescued by simultaneous overexpression of Chip. Eye-antennal discs in which *UAS-HA-Chip* (A–D), *UAS-Notch-ICD* (F–I), and both *UAS-HA-Chip* and *UAS-Notch-ICD* (K–N) were overexpressed using *ey-GAL4* driver showing Elav expression. Note that Elav staining of *ey-GAL4*–driven larval eye discs having co-overexpression of *Notch-ICD* and *Chip* (K-N) showed reduced defects in ommatidial spacing and fusion compared to only *Notch-ICD* overexpressing discs (F–I). Images presented in C, H, and M are merged images of those presented in A and B, F and G, and K and L, respectively. Images presented in D, I, and N are high-magnification images of Elav expressing cells shown in B, G, and L, respectively. Scale bars for A–C, F–H, and K–M, 50 μm and for D, I, and N, 5 μm. (E, J, and O) Nail polish imprints of adult eyes of genotypes as in A–D, F–I, and K–N, respectively. Note the co-expression of *Notch-ICD* and *Chip* showed a considerable rescue of the adult eyes phenotype with normal sized and less fused ommatidia (O) compared to only *Notch-ICD* overexpressing eye (J). (P) Histograms show mean number of cells in one eye disc of different genotypes: *ey-GAL4/+* (grey), *ey-GAL4/+; UAS-Notch-ICD/+* (pink), and *ey-GAL4/UAS-HA-Chip; UAS-Notch-ICD/+* (blue). Note that eye disc, in which both *Notch-ICD* and *Chip* (blue) were co-overexpressed, contains a fewer number of cells compared to the disc in which only *Notch-ICD* (pink) was overexpressed. (Q) Fold change in expression levels of the indicated genes between *Notch-ICD* and *Chip* overexpressing eye discs and only *Notch-ICD* expressing eye discs using *ey-GAL4* driver as determined by quantitative real-time PCR. Error bars indicate standard error of the mean of three replicates.

antibody, we found that the number of mitotic cells expressing phospho-Histone H3 is more in *Notch-ICD* overexpressing disc, and the disc, where both *Notch-ICD* and *Chip* were overexpressed, showed a fewer number of mitotic cells, which is comparable to wild-type (see supplementary Fig. 1). Phalloidin staining clearly showed that F-actin was disorganized in only *Notch-ICD* overexpressing eye disc, whereas F-actin organization was comparable to wild-type in the eye disc from both *Notch-ICD* and *Chip* overexpressing individuals (see supplementary Fig. 1). These results revealed that phenotypes caused by Notch overexpression are sensitive to the dosage of Chip.

4. Discussion

4.1. Chip is a novel interacting partner of Notch

Genetic and molecular analyses revealed that Notch signaling plays major role in the establishment of distinct developmental cell lineages. Its role in *Drosophila* wing margin formation has been evident since the time of first identification of Notch mutant. Here, we report the physical interaction between Notch and cofactor Chip proteins. In addition, Chip and Notch showed strong genetic interactions. It is worth mentioning that Notch and Chip share many common features: (i) mutations in both *Notch* and *Chip* are haploinsufficient, (ii) Notch-ICD and Chip contain nuclear localization signals and they are localized in the nucleus, (iii) both Notch-ICD and Chip act as cofactors for transcription, and (iv) Notch and Chip functions are highly dosage sensitive. To the best of our knowledge, the present study demonstrated for the first time that Notch-ICD and Chip proteins directly bind and confirm a functional relationship between Notch and Chip, consistent with their molecular interactions.

4.2. Correct amount of Chip is required for normal function of Notch at the DV boundary for wing margin formation, and Notch function in DV boundary is presumably mediated by the Notch–Chip heterodimer

Different models have been proposed to explain the establishment of affinity difference of dorsal and ventral cells in the DV boundary and its maintenance. One model proposes that in addition to its role in Notch signaling, Fringe can generate an affinity difference between dorsal and ventral cells in DV boundary in a Notch-independent manner [51,52]. Another model suggests that Notch activity is sufficient to establish an affinity difference between dorsal and ventral cells in DV boundary [22,53]. The third model proposes that Ap controls the expression of surface proteins in dorsal and ventral cells, and these surface proteins form complexes with activated Notch that results in dorsal or ventral affinity state [39]. According to this model, the role of Ap is instructive, and Notch activity is essential but permissive [39]. Although all these models explain whether Notch activity can generate a dorsal or ventral affinity state on its own, there is no question about the essential role of Notch activity in the maintenance of DV boundary, resulting in wing margin formation.

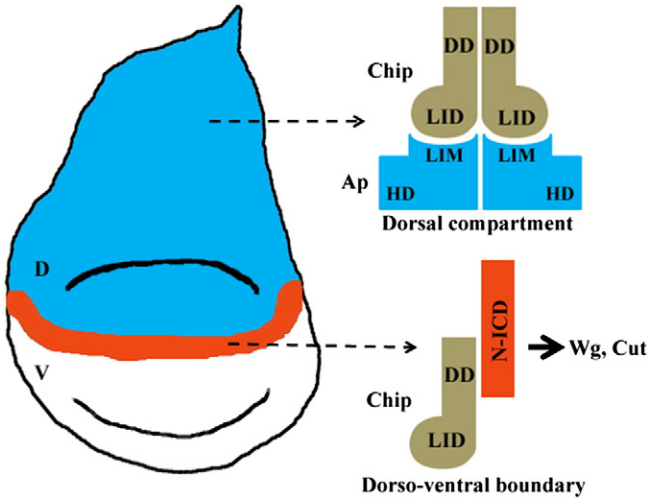

Fig. 8. A model for Notch–Chip function in DV boundary of wing disc. As shown earlier, two Ap molecules and two Chip molecules form a functional tetrameric complex in the dorsal compartment of wing disc (see refs. [25,27,28,30]). Here, we show that in the DV boundary, a Notch–Chip dimer may be the functional complex for executing the Notch function through expression of downstream target genes such as Wg and Cut.

We found that overexpression of Chip in different domains of the wing disc resulted in loss of Notch activity in DV boundary area, as evident by significant reductions or complete loss of Wg or Cut expression without affecting the expression and distribution of Notch protein in the DV boundary area and, consequently, the wing margin loss in adult wing. Probably, overexpression of Chip facilitates dimerization of Chip molecules and it limits heterodimer formation with endogenous Notch molecules, which ultimately leads to this kind of DV boundary defect phenotype. Moreover, overexpression of Chip in the DV boundary can rescue the wing margin loss phenotype caused by overexpression of activated Notch in this domain. Simultaneous co-overexpression of Notch-ICD and Chip may result in Notch–Chip heterodimer formation, which presumably restores the normal DV boundary area leading to normal wing margin formation. Taken together, our findings are consistent with the hypothesis that the relative amounts of Notch and Chip are important for DV boundary formation in the wing disc.

A dimer of Chip bridges two Ap molecules to form an active tetrameric complex *in vivo* [27,28,30]. This complex binds with DNA through the homeodomain of Ap to turn on the Ap target genes required for dorsal compartmentalization of the wing disc. In the present study, we determined that Notch directly interacts with the dimerization domain of Chip. It is intriguing to speculate that Notch function in the DV boundary area is mediated by the Notch–Chip heterodimer. Our results showed that only full-length Chip or *Chip*-ΔLID but not the *Chip*-Δ*DD* expression were able to rescue the wing margin phenotype generated by overexpression of Notch-ICD. These results support the idea that Notch function in the DV boundary area is presumably dependent on Notch–Chip heterodimer formation (Fig. 8). Our analysis neither excluded the possibility that additional proteins might also take part along with this Notch–Chip heterodimer for executing the Notch function in the DV boundary nor did it address whether Notch and Ap compete for binding to their common cofactor Chip in the DV boundary region.

It has previously been shown that the GATA factor Pannier binds to Chip monomer, and Chip acts as a bridge between Achaete/Scute-Daughterless heterodimer bound to the E boxes of Achaete promoter and Pannier bound to the GATA sites of dorso-central (DC) enhancer to allow enhancer–promoter interactions, resulting in the activation of proneural genes [54,55]. A dimer of Chip binds two Ap molecules to form an active tetrameric complex for its function; here, these data showed that proteins such as Pannier could interact with Chip monomer.

4.3. Chip overexpression can suppress Notch-induced cell proliferation

In addition to its combinatorial role with Notch in DV boundary formation, overexpression of Chip can also rescue Notch-induced cell proliferation in wing imaginal discs. The tumorous wing discs, caused by overexpression of activated form of Notch, were found to attain significantly reduced size when Chip was also present in excess. We found that the expression levels of *p53* and *dMyc* were upregulated, while that of *deadpan* and *string/cdc25* were downregulated in both *Notch-ICD* and *Chip* expressing discs compared to *Notch-ICD* expressing discs only. These differential expressions of cell cycle regulators may play some role in reducing the size of the disc, where both *Notch-ICD* and *Chip* are co-overexpressed. Although our analysis could not provide the exact mechanism by which excess Chip can rescue the proliferative

effects of Notch-ICD overexpression, we presume that excess Chip would probably lead to the titration of overexpressed Notch-ICD, inhibiting the effects of Notch signals on cell proliferation.

Supplementary data to this article can be found online at http://dx.doi.org/10.1016/j.bbagen.2014.12.026.

Acknowledgements

The authors wish to thank Spyros Artavanis-Tsakonas, Donald J. van Meyel, and the Bloomington Stock Center for numerous fly stocks. Some of the antibodies used in this work were obtained from the Developmental Studies Hybridoma Bank, Iowa, USA. We would also like to acknowledge the help from DST-Confocal facility in BHU for confocal microscopy. N.S. was supported by a fellowship from Indian Council of Medical Research (ICMR), India. This work was supported by grants from Department of Biotechnology (DBT), India to A.M. and M.M.

References

[1] E.R. Andersson, R. Sandberg, U. Lendahl, Notch signaling: simplicity in design, versatility in function, Development 138 (2011) 3593–3612.
[2] S. Artavanis-Tsakonas, M.D. Rand, R.J. Lake, Notch signaling: cell fate control and signal integration in development, Science 284 (1999) 770–776.
[3] M.E. Fortini, Notch signaling: the core pathway and its posttranslational regulation, Dev. Cell 16 (2009) 633–647.
[4] K.G. Guruharsha, M.W. Kankel, S. Artavanis-Tsakonas, The Notch signalling system: recent insights into the complexity of a conserved pathway, Nat. Rev. Genet. 13 (2012) 654–666.
[5] J. Liu, C. Sato, M. Cerletti, et al., Notch signaling in the regulation of stem cell self-renewal and differentiation, Curr. Top. Dev. Biol. 92 (2010) 367–409.
[6] O.L. Mohr, Character changes caused by mutation of an entire region of a chromosome in *Drosophila*, Genetics 4 (1919) 275–282.
[7] T.H. Morgan, C.B. Bridges, Sex-linked inheritance in Drosophila, Publs. Carnegie Instn., 237, 1916, pp. 1–88.
[8] K.A. Wharton, K.M. Johansen, T. Xu, et al., Nucleotide sequence from the neurogenic locus Notch implies a gene product that shares homology with proteins containing EGF-like repeats, Cell 43 (1985) 567–581.
[9] C.M. Blaumueller, H. Qi, P. Zagouras, et al., Intracellular cleavage of Notch leads to a heterodimeric receptor on the plasma membrane, Cell 90 (1997) 281–291.
[10] C. Brou, F. Logeat, N. Gupta, A novel proteolytic cleavage involved in Notch signaling: the role of the disintegrin-metalloprotease TACE, Mol. Cell 5 (2000) 207–216.
[11] B. De Strooper, W. Annaert, P. Cupers, et al., A presenilin-1-dependent gamma-secretase-like protease mediates release of Notch intracellular domain, Nature 398 (1999) 518–522.
[12] G. Struhl, I. Greenwald, Presenilin is required for activity and nuclear access of Notch in *Drosophila*, Nature 398 (1999) 522–525.
[13] Y. Ye, N. Lukinova, M.E. Fortini, Neurogenic phenotypes and altered Notch processing in *Drosophila* presenilin mutants, Nature 398 (1999) 525–529.
[14] N. Sachan, A.K. Mishra, M. Mutsuddi, A. Mukherjee, The *Drosophila* importin-α3 is required for nuclear import of Notch in vivo and it displays synergistic effects with Notch receptor on cell proliferation, PLoS One 8 (2013) e68247.
[15] J.A. Campos-Ortega, Mechanisms of early neurogenesis in *Drosophila melanogaster*, J. Neurobiol. 24 (1993) 1305–1327.
[16] M.E. Fortini, S. Artavanis-Tsakonas, The suppressor of hairless protein participates in Notch receptor signaling, Cell 79 (1994) 273–282.
[17] L. Wu, J.C. Aster, S.C. Blacklow, et al., MAML1, a human homologue of *Drosophila* mastermind, is a transcriptional co-activator for NOTCH receptors, Nat. Genet. 26 (2000) 484–489.
[18] M. Baron, H. Aslam, M. Flasza, et al., Multiple levels of Notch signal regulation, Mol. Membr. Biol. 19 (2002) 27–38.
[19] A. Mukherjee, A. Veraksa, A. Bauer, et al., Regulation of Notch signalling by non-visual β-arrestin, Nat. Cell Biol. 7 (2005) 1191–1201.
[20] C. Bourgouin, S.E. Lundgren, J.B. Thomas, Apterous is a *Drosophila* LIM domain gene required for the development of a subset of embryonic muscles, Neuron 9 (1992) 549–561.
[21] B. Cohen, M.E. McGuffin, C. Pfeifle, et al., Apterous, a gene required for imaginal disc development in Drosophila encodes a member of the LIM family of developmental regulatory proteins, Genes Dev. 6 (1992) 715–729.
[22] S.S. Blair, Cell lineage: compartments and capricious, Curr. Biol. 11 (2001) R1017–R1021.
[23] F. Diaz-Benjumea, S.M. Cohen, Interaction between dorsal and ventral cells in the imaginal disc directs wing development in *Drosophila*, Cell 75 (1993) 741–752.
[24] J.A. Williams, S.W. Paddock, S.B. Carroll, Pattern formation in a secondary field: a hierarchy of regulatory genes subdivides the developing *Drosophila* wing disc into discrete subregions, Development 117 (1993) 571–584.
[25] P. Fernandez-Funez, C.H. Lu, D.E. Rincon-Limas, et al., The relative expression amounts of apterous and its co-factor dLdb/Chip are critical for dorso-ventral compartmentalization in the *Drosophila* wing, EMBO J. 17 (1998) 6846–6853.
[26] P. Morcillo, C. Rosen, M.K. Baylies, et al., Chip, a widely expressed chromosomal protein required for segmentation and activity of a remote wing margin enhancer in *Drosophila*, Genes Dev. 11 (1997) 2729–2740.
[27] D.E. Rincon-Limas, C.H. Lu, I. Canal, et al., The level of DLDB/CHIP controls the activity of the LIM homeodomain protein apterous: evidence for a functional tetramer complex in vivo, EMBO J. 19 (2000) 2602–2614.
[28] D.J. van Meyel, D.D. O'Keefe, L.W. Jurata, et al., Chip and Apterous physically interact to form a functional complex during *Drosophila* development, Mol. Cell 4 (1999) 259–265.
[29] U. Weihe, M. Milan, S.M. Cohen, Regulation of Apterous activity in *Drosophila* wing development, Development 128 (2001) 4615–4622.
[30] M. Milan, S.M. Cohen, Regulation of LIM homeodomain activity in vivo: a tetramer of dLDB and apterous confers activity and capacity for regulation by dLMO, Mol. Cell 4 (1999) 267–273.
[31] D.J. van Meyel, D.D. O'Keefe, S. Thor, et al., Chip is an esssential cofactor for Apterous in the regulation of axon guidance in *Drosophila*, Development 127 (2000) 1823–1831.
[32] P. Hari, M. Deshpande, N. Sharma, et al., Chip is required for posteclosion behaviour in *Drosophila*, J. Neurosci. 28 (2008) 9145–9150.
[33] J.Y. Roignant, K. Legent, F. Janody, et al., The transcriptional co-factor Chip acts with LIM-homeodomain proteins to set the boundary of the eye field in *Drosophila*, Development 137 (2010) 273–281.
[34] F.J. Diaz-Benjumea, S.M. Cohen, Serrate signals through Notch to establish a Wingless-dependent organizer at the dorsal/ventral compartment boundary of the *Drosophila* wing, Development 121 (1995) 4215–4225.
[35] K.D. Irvine, Fringe, Notch, and making developmental boundaries, Curr. Opin. Genet. Dev. 9 (1999) 434–441.
[36] M. Milan, S.M. Cohen, Temporal regulation of Apterous activity during development of the *Drosophila* wing, Development 1 (2000) 3069–3078.
[37] J.F. de Celis, A. Garcia-Bellido, S.J. Bray, Activation and function of Notch at the dorsal-ventral boundary of the wing imaginal disc, Development 122 (1996) 359–369.
[38] D. Doherty, G. Fenger, S. Younger-Shepherd, et al., Dorsal and ventral cells respond differently to the Notch ligands Delta and Serrate during *Drosophila* wing development, Genes Dev. 10 (1996) 421–434.
[39] M. Milan, S.M. Cohen, A re-evaluation of the contributions of Apterous and Notch to the dorsoventral lineage restriction boundary in the *Drosophila* wing, Development 130 (2003) 553–562.
[40] R.J. Fleming, Y. Gu, N.A. Hukriede, Serrate-mediated activation of Notch is specifically blocked by the product of the gene fringe in the dorsal compartment of the *Drosophila* wing imaginal disc, Development 124 (1997) 2973–2981.
[41] D.J. Moloney, V.M. Panin, S.H. Johnston, et al., Fringe is a glycosyltransferase that modifies Notch, Nature 406 (2000) 369–375.
[42] S. Munro, M. Freeman, The Notch signalling regulator fringe acts in the Golgi apparatus and requires the glycosyltransferase signature motif DXD, Curr. Biol. 10 (2000) 813–820.
[43] M. Milan, F.J. Diaz-Benjumea, S.M. Cohen, *Beadex* encodes an LMO protein that regulates Apterous LIM–homeodomain activity in *Drosophila* wing development: a model for *LMO* oncogene function, Genes Dev. 12 (1998) 2912–2920.
[44] C. Zeng, N.J. Justice, S. Abdelilahm, et al., The *Drosophila* LIM-only gene, dLMO, is mutated in Beadex alleles and might represent an evolutionarily conserved function in appendage development, Proc. Natl. Acad. Sci. U. S. A. 95 (1998) 10637–10642.
[45] P. Morcillo, C. Rosen, D. Dorsett, Genes regulating the remote wing margin enhancer in the *Drosophila* cut locus, Genetics 144 (1996) 1143–1154.
[46] W. Helms, H. Lee, M. Ammerman, et al., Engineered truncations in the *Drosophila* mastermind protein disrupt Notch pathway function, Dev. Biol. 215 (1999) 358–374.
[47] M.W. Kankel, G.D. Hurlbut, G. Upadhyay, et al., Investigating the genetic circuitry of mastermind in *Drosophila*, a Notch signal effector, Genetics 177 (2007) 2493–2505.
[48] T. Xu, G.M. Rubin, Analysis of genetic mosaics in developing and adult *Drosophila* tissues, Development 117 (1993) 1223–1237.
[49] A.H. Brand, N. Perrimon, Targeted gene expression as a means of altering cell fates and generating dominant phenotypes, Development 118 (1993) 401–415.
[50] M.J. Go, D.S. Eastman, S. Artavanis-Tsakonas, Cell proliferation control by Notch signaling in *Drosophila* development, Development 125 (1998) 2031–2040.
[51] D.D. O'Keefe, J.B. Thomas, *Drosophila* wing development in the absence of dorsal identity, Development 128 (2001) 703–710.
[52] C. Rauskolb, T. Correia, K.D. Irvine, Fringe-dependent separation of dorsal and ventral cells in the *Drosophila* wing, Nature 401 (1999) 476–480.
[53] C.A. Micchelli, S.S. Blair, Dorsoventral lineage restriction in wing imaginal discs requires Notch, Nature 401 (1999) 473–476.
[54] P. Heitzler, L. Vanolst, I. Biryukova, et al., Enhancer–promoter communication mediated by Chip during Pannier-driven proneural patterning is regulated by Osa, Genes Dev. 17 (2003) 591–596.
[55] P. Ramain, R. Khechumian, K. Khechumian, et al., Interactions between Chip and the Achaete/Scute–daughterless heterodimers are required for Pannier-driven proneural patterning, Mol. Cell 6 (2000) 781–790.